RSC Advances

PAPER

View Article Online
View Journal | View Issue

Cite this: *RSC Adv.*, 2024, **14**, 31598

Sequential effects of two cations on the fluorescence emission of a coordination polymer with Zn_4O core in node†

Jagajiban Sendh and Jubaraj B. Baruah *

Distinct changes in the fluorescence emissions of free ligand 5-(1,3-dioxo-1*H*-benzo[de]isoquinolin-2(3*H*)-yl)isophthalic acid (**H_2NAPHISO**) than a 2D-zinc-coordination polymer of it, caused by sequential interactions with different sets of binary cations were observed. The coordination polymer having unsymmetrical Zn_4O core of tetranuclear zinc-node could be dispersed in dimethylformamide without its degradation. The coordination polymer had an emission peak at 435 nm (quantum yield = 0.082) which was selectively quenched by adding Fe^{2+} ions. Based on this quenching, the Fe^{2+} ions in aqueous solution could be detected with a detection limit 42.57 nM. The metal ions such as Li^+, Na^+, Cd^{2+}, Hg^{2+}, Al^{3+} did not interfere in the detection; but each of these ions together with Fe^{2+} ions showed characteristic shift of the emission spectra. The **H_2NAPHISO** in dimethyl formamide was non-fluorescent, but showed emission at 452 nm upon addition of Cd^{2+} or Zn^{2+} ions. This new emission of **H_2NAPHISO** caused by zinc or cadmium ions was not quenched by Fe^{2+} ions. Various cations had affected the emission of the **H_2NAPHISO** with Zn^{2+} which was much different from the corresponding changes caused by the same ion on the emission of the coordination polymer. For example, the Mn^{2+} and Zn^{2+} ions together in a solution of the ligand showed a broad emission spectrum spreading over 380–450 nm, but ions Sn^{2+} and Zn^{2+} together had showed emission at a shorter wavelength (380 nm). These allowed to modulate the emission of the ligand by binary combination of metal ions.

Received 1st September 2024
Accepted 26th September 2024

DOI: 10.1039/d4ra06309k

rsc.li/rsc-advances

Introduction

The amounts as well as variety of metal ions present in water in different sources, such as drinking-water, natural-water, laboratory solutions or even in a health tonic differ. Utility oriented products such as alloys, semiconductors often contain trace quantities multiple metal ions that requires detections and estimation. Simple organic sensing molecules are often designed for selective fluorescence detection of metal ions,[1] but there remain limitations when than one or more ions interfere in the detection processes. Fluorescent sensor array is an alternate method for detections of multiple ions, the method is based on pattern recognition. There is necessity to identify new arrays with tuneable emission over a wide range of wavelengths and also such arrays must work in real time with high efficiencies.[2] The metal complexes having diverse emission properties provide examples for fluorescence applications from materials to biology[3] and some studies have provided essence to distinguish various metal ions without interference of other.[4] Beyond these aspects, thermally enhanced delayed fluorescence, supramolecular effects are other processes for distinction of analytes.[5] The 1,8-naphthalimide together with different amounts 1,3-benzenedicarboxylic acid had shown promise to tune emission[6] and 1,3-benzenedicarboxylic acid linked 1,8-naphthalimides is well known to form metal complexes.[7] On the other hand, due to differences in the structural flexibility and response to external stimuli, such as solvent, pH *etc.*, the guest binding by a fluorescent dicarboxylic acid differs from their respective metal complexes. A metal complex also involves second coordination sphere to bind a guest in a much different manner than a free ligand. Hence, there is a necessity to study the comparative guest binding abilities of a ligand with its metal complex. The naphthalimide derived chemo-sensors have been used in ion and molecular recognitions and extended to biological systems.[8] Their established metal complexes[9] or framework structures,[10] emission properties[11] have significance in material design. Π-stacks among naphthalimide rings guide self-assemblies of metal complexes.[12] On the other hand, the nodes of zinc coordination polymers modulate physiochemical properties.[13] Hence, there is scope to study zinc coordination polymers possessing mono-,[14] bi-,[15] tri-,[16] tetra-,[17] penta-,[18] hexa-,[19] hepta-,[20] octa-nuclear[21] node (listed in the Fig. S1 of ESI†).

Department of Chemistry, Indian Institute of Technology Guwahati, Guwahati-781 039, Assam, India. E-mail: juba@iitg.ac.in; Tel: +91-361-2582311

† Electronic supplementary information (ESI) available: The EDX, thermogravimetry, fluorescence and UV-visible plots, Crystallographic table, fluorescence lifetime profiles, are available in supporting information. CCDC 2377351. For ESI and crystallographic data in CIF or other electronic format see DOI: https://doi.org/10.1039/d4ra06309k

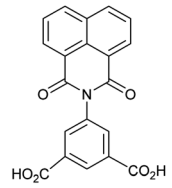

5-(1,3-dioxo-1*H*-benzo[*de*]isoquinolin-2(3*H*)-yl)isophthalic acid

Fig. 1 Structure of the H_2NAPHISO.

Robust nanocages of zinc carboxylate with mixed tri-nuclear and tetra-nuclear nodes known in literature has interesting emission properties, which further widens the scopes.[22]

The properties of a coordination polymers are also dependent on nodes, for example, Zn_4O-based carboxylate of 1,4-benzene dicarboxylic acid has high surface-area;[17d] and the optical property of nanocage of zinc-carboxylate are modulated by Eu^{3+}/Tb^{3+} ions.[22] Some coordination polymers have multiple nodes,[16d] and some having similar nodes have differences in structures.[17a,e] A recent report depicted 1D- as well as 3D-zinc dicarboxylate coordination polymers of 5-(1,3-dioxo-1*H*-benzo [de] isoquinolin-2(3*H*)-yl)isophthalic acid (abbreviated as **H_2-NAPHISO** Fig. 1),[23] but there exist further possibilities to explore new naphthalimide decorated zinc-carboxylate nodes. The fluorescence-based detections of ions are generally performed based on mechanism,[24] hence, insight on interactions of different ions influencing free ligand as well as coordinated ligands are essential. We have studied here a new zinc coordination polymer of the above ligand with naphthalimide decorated nodes and explored cation sensing properties. The **H_2NAPHISO** has two carboxylic acid groups, directed in 120° to serve as linkers to anchor multiple metal ions in coordination polymers that conventionally observed in the framework structures of isophthalic acid.[25]

Experimental

Materials and methods

Infra-red spectra of the solid samples were recorded with a PerkinElmer spectrometer by attenuated total reflectance method. Powder X-ray diffraction patterns of finely grounded samples were recorded on 9 KW Rigaku Smartlab (Japan) X-ray powder diffractometer. Thermogravimetric studies were carried out on a PerkinElmer instrument with a heating rate of 10 ° C min^{-1} under a nitrogen atmosphere. For optical microscopic images of crystals, the crystals were placed on glass slide and images were recorded by an Olympus (Japan) optical microscope. Scanning electron micrographs were performed on a Sigma 300 FE-SEM instrument (Carl Zeiss, Germany) by spreading powder sample on a carbon tape. UV-visible spectra of different solutions (3 mL of specific concentration) taken in a quartz cuvette were recorded on a PerkinElmer UV-visible spectrophotometer (model Lambda 365+, USA). Fluorescence emission spectra were recorded at room temperature by using the Horiba Jobin Yvon Fluoromax-4 (France) spectrofluorometer. Picosecond time-resolved and steady state Luminescence were performed on an Edinburg instrument (UK), Lifespec II equipment. The nuclear magnetic resonance spectra were recorded by using a 600 MHz Bruker (Germany) instrument. The tetramethyl silane was used as internal standard. Cyclic voltammograms were recorded by a CHI6044E potentiostat (USA) equipped with three-electrodes. Each measurement was carried out with 1 mM solution (10 mL) of respective solution in *N*,*N*′-dimethylformamide with glassy carbon electrode as the working electrode, platinum as the counter electrode, and Ag/$AgNO_3$ as the reference electrode with scan rate of 100 mV s^{-1}. To compensate internal resistance tetra-butyl ammonium perchlorate was used as supporting electrolyte. The quantum yield of the **H_2NAPHISO** was calculated by comparing the mission area with the quinine sulphate as standard. The specific surface-area for N_2 sorption at −196 °C of the coordination polymer was done by using a Quantachrome Autosorb iQMP gas sorption analyzer. For the BET surface area analysis the samples were prepared by stirring the coordination polymer in water for 6 h and then it was dried in oven at 100 °C for 5 h.

The ligand **H_2NAPHISO** was prepared by literature procedure.[26]

Synthesis and characterisation of the Zn_4O-CP

A mixture of **H_2NAPHISO** (72 mg, 0.2 mmol) and zinc(II) acetate hexahydrate (80 mg, 0.4 mmol) was dissolved in warm DMF (20 mL). The solution was taken in a Teflon coated hydrothermal vessel. The vessel was closed and placed on an autoclave set at 100 °C. The solvothermal reaction was allowed to continue with constant heating for 36 hs. Then it was allowed to attain room temperature, which resulted in plate-like crystals settled at the bottom of the vessel. The supernatant solution was decantated and crystals were collected. Single crystal X-ray structure of a suitable crystal was determined. The composition was established by EDX and bulk purity of the crystals were determined by powder X-ray technique. Isolated yield: 70% (based on Zn). IR: 1661 (s, $\nu_{C=O,\ carboxylate}$), 1710 (s, $\nu_{C=O,\ imide}$).

Single-crystal X-ray diffraction data for the zinc-coordination polymer was collected by using MoKα radiation ($\lambda = 0.71073$ Å, 297 K) by a Brucker Nonius SMART APEX CCD diffractometer equipped with a graphite monochromator and an Apex CCD camera. Data reduction and cell refinement were performed by using SAINT and XPREP software. The structure was solved by direct method and refined by full-matrix least squares on F^2 using SHELXL-2018 software. The hydrogen atoms were refined in isotropic approximation after placing them at the respective geometrical positions by riding. The non-hydrogen atoms were refined by anisotropic approximation against F^2 of all the reflections. The crystal and structural parameters are listed in Table S1.† A naphthalimide ring and a DMF molecule had crystallographic disorder, the disorders were resolved by sharing the disordered atoms at independent positions and were refined isotopically.

Limit of detection (LOD)

The LOD of the **Zn_4O-CP** in the detection of Fe^{2+} was carried out by measuring the fluorescence emission intensity after lapse of

one-minute time for ten-times. From these measurements, the standard deviation (σ) was calculated by using equation $\sigma = \sqrt{\Sigma(x_i - \mu)^2/N}$. ($x_i$ is the intensity of the **Zn_4O-CP**), μ is mean intensities of those, N is the total numbers of measurements. The fluorescence emission intensities with increase in the concentrations of the ions were plotted and the LOD was calculated from $3\sigma/k$ (k is the slope of the calibration curve).

Results and discussion

Structural study

A 3D coordination polymer [Zn(NAPHISO)$(DMF)_{1.5}$] possessing binuclear Zn^{2+} clusters[16] was reported from the zinc(II) acetate dihydrate and **H_2NAPHISO** in *N*,*N*-dimethylformamide (DMF), whereas, the same reaction in DMSO provided a zinc coordination polymer with mononuclear node. We find that in solvothermal condition in DMF, a previously not reported 2D-zinc coordination polymer was exclusively formed. It had a composition $[Zn_4O(NAPHISO)_3(DMF)_2]_n$ confirmed by elemental percentages ascertained by energy dispersive X-ray analysis from field emission scanning electron microscopy (FE-SEM) (Fig. S3†). The experimental atomic percent of the coordination polymer had tallied with the composition of the structure of the **Zn_4O-CP** observed from single crystal X-ray diffraction. From the unit cells parameters of the single crystals of the **Zn_4O-CP** were found to belong to triclinic $P\bar{1}$ space group. A node of the coordination polymer is shown in the Fig. 2a. It was comprised of four zinc ions centrally linked to an oxide ion through μ^4-binding mode of oxide. The carboxylate groups of each **NAPHISO** were uniformly coordinated to the zinc ions through η^2-bridging mode. The coordination polymer had two symmetry related chains growing independently having inversion centre having symmetry operation relation (i) x, y, z and (ii) $-x, -y, -z$. The Zn_4O cores were observed in polynuclear complexes as well as coordination polymers usually are associated with interesting optical properties, and those were suggested to be structural analogue of zinc-oxide.[12] There was one zinc ion that had octahedral environment, whereas rest were in tetrahedral environments. The octahedral zinc ion had four oxygen atoms from independent carboxylates occupying square-planar positions. Whereas, the oxygen of oxide as well as the oxygen of DMF coordinated at the other two sites of octahedral geometry were at a *trans*-disposition to each other. The two tetrahedral zinc sites (Zn_1 and Zn_3) had three oxygens of carboxylate coordinating at three site and fourth site (Zn_4) was with the oxygen of oxide, whereas the third tetrahedral zinc environment was created by having three oxygen of carboxylates and an oxygen of DMF. There were two coordinated DMF molecules per node. One DMF molecule was bound to the hexa-coordinate zinc ion (Zn_2) and other was bound to the tetra-coordinate zinc ion (Zn_4) (Fig. 2a). Metal–organic frameworks with tetranuclear zinc nodes generally have the tetrahedral zinc-sites equivalent with bridging carboxylates and coordinating oxide.[17a–c]

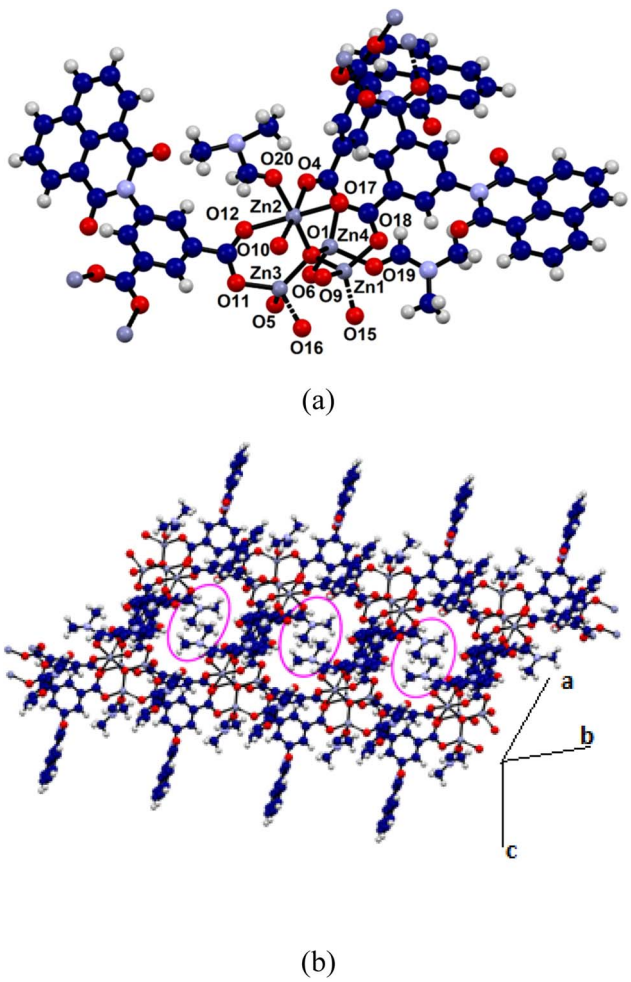

Fig. 2 (a) A node of the Zn_4O-CP (50% thermal ellipsoids); (b) 2D-structure showing the coordinated DMF molecules in the encircled spaces.

The **Zn_4O-CP** had dissimilar coordination environments in the nodes which is different from the tetranuclear nodes of zinc complexes available in literature.[15] In the present case, the **Zn_4O-CP** formed a 2-dimensional sheet-like arrangements (Fig. 2b) by utilising two symmetry related chains (symmetry of inversion) of the coordination polymers, and it had enclosures suitable to accommodate the hydrophobic portions of the DMF molecules within those (encircled in Fig. 2b). The metal ligand bonds, Zn_4–O_{19} 1.994(5) Å and Zn_2–O_{12}, 2.011(4) Å distances had suggested strong binding of the two solvent molecules. On the other hand, the four Zn–O bonds linking the zinc ions with the central oxide ion were 1.941(3) Å, 2.013(3) Å, 1.923(3) Å and 1.905(3) Å, showing that each zinc ion was held tightly to the central oxide. On the other hand, the Zn–O bonds of the carboxylates bonded in μ^2: η^1 η^1 manner varied from 1.929(4) Å–2.279(4) Å showing the peripheral knitting of the core by the carboxylate groups. The shortest distance between the two parallel planes of the naphthalimide rings was 10.36 Å in the coordination polymer; hence, it did not have π-interactions among them.

Microscopic, infra-red spectroscopic, surface-area and thermal studies

The phase-purity of the **Zn_4O-CP** was determined by comparing the X-ray powder diffraction pattern of the coordination

polymer with the simulated powder X-ray diffraction pattern obtained from the crystallographic information file (Fig. S2a†). The scanning electron micrograph of the coordination polymer showed plate-like shapes (Fig. S4†), which was in accordance of 2D-structure of the coordination polymer.

The FT-IR spectra of the **H_2NAPHISO** and **Zn_4O-CP** are shown in Fig. S2b.† The carbonyl C=O of the imide and carboxylic acid group of the ligand appeared as a sharp peak at 1667 cm^{-1} and 1694 cm^{-1}. The carboxylate O–H of the ligand appeared as a broad peak in the region 2500–3000 cm^{-1}. The C=O stretches of the **Zn_4O-CP** were observed at 1661 cm^{-1} and 1668 cm^{-1} respectively. Carbonyl group of the naphthalimide group appeared at 1710 cm^{-1}. The amide carbonyl of the two independent dimethylformamide were at 1589 cm^{-1} and 1576 cm^{-1}.

The coordination polymer was found to decompose at 420 °C. The coordination polymer had lost the DMF molecules in range of 100–320 °C (11% loss, showing 2.3 molecules of DMF loss per node), and the other ligands were decomposed sharply at 420 °C to 600 °C to loss 82.5% of its weight forming zinc oxide (Fig. S6†). The surface-area determined from nitrogen adsorption isotherm (Fig. S7†) was 13.367 $m^2\ g^{-1}$ and it had a pore volume of $4.895 \times 10^{-3}\ cm^3\ g^{-1}$ at $p/p_0 = 0.5$. The average pore radius was found to be 1.77 Å. The desorption of the nitrogen followed the same path as of the adsorption profile, accordingly, there was no hysteresis, showing a physisorption of the nitrogen in the interstitial pores.

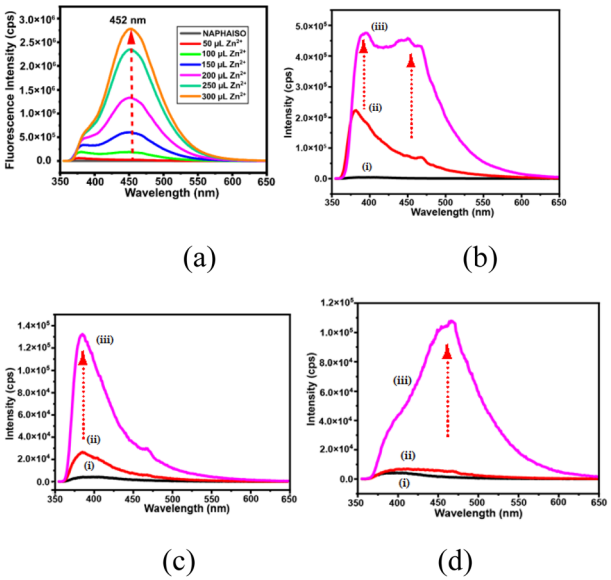

Fig. 3 Fluorescence emission spectra of a solution of H_2NAPHISO (3 mL, 1 mM in DMF) (λ_{ex} = 333 nm) (a) by adding different aliquots (50 μL, 10 mM Zn^{2+} solution in water). The emission spectra of (b–d) (i) **H_2-NAPHISO**, and by adding solutions of (b) (ii) Mn^{2+}, (iii) followed by Zn^{2+} ions, (c) (ii) Sn^{2+}, (iii) followed by Zn^{2+} and (d) (ii) Fe^{2+}, (iii) followed by Zn^{2+} ions (in b–d, 300 μL of 10 mM solution of the respective metal ions in water).

Effect of divalent metal ions on the fluorescence spectra of H_2NAPHISO

There are large numbers of fluorophores that are utilised to distinguish and selectively detect Zn^{2+} or Cd^{2+} ions.[27] Many of fluorescence sensing coordination polymers were sensitive to both ions with d^{10} electronic configuration due to metal to ligand charge-transfer transitions.[28] Some sensing molecules make distinctions of ions like Zn^{2+} and Al^{3+} by emitting at different wavelengths,[29] or some also distinguishes Zn^{2+} and Cd^{2+} ions through characteristic emissions;[30] but the combined effects of ions are yet to be detailed. The **H_2NAPHISO** in DMF showed insignificant fluorescence emission at 452 nm upon excitation at 335 nm. However, addition of an aqueous solution of Zn^{2+} caused a 300-fold increase in the emission intensity (Fig. 3a). A similar effect was also observed upon addition of Cd^{2+} ions. However, the emission intensity changes caused by several cations such as Li^+, Na^+, K^+, Cs^+, Mg^{2+}, Hg^{2+} or Al^{3+} on the emission ON caused by Zn^{2+} ions on the **H_2NAPHISO** were not significant, but some other ions had characteristic features, that may have withstanding implications. The cations like, Mn^{2+}, Sn^{2+} and Fe^{2+} had interfered in the emission and each had showed characteristic emission features. There was a weak emission peak at 380 nm of **H_2NAPHISO** with Mn^{2+} ions (Fig. 3b); this emission peak at 380 nm was observed as a shoulder in the spectra of the solution of **H_2NAPHISO** with Zn^{2+} ions without the Mn^{2+} ions. But, addition of Zn^{2+} ions to a solution of **H_2NAPHISO** containing Mn^{2+} ions had showed enhancement of intensities at both the wavelengths (at 380 nm and 452 nm). That is to suggest that the emission had spread over a broader wavelength spreading over 380 nm to 452 nm. Such an observation was reported by us in the case of a naphthalimide derivative showing white light emission when binary component of metal ions was present in solution.[31] On the other hand, addition of a solution of Sn^{2+} to **H_2NAPHISO** showed fluorescence emission at 380 nm (Fig. 3c), to the same solution addition of Zn^{2+} had enhanced the intensity of this peak, without showing an additional emission. Furthermore, the Fe^{2+} ions with a solution of **H_2NAPHISO** was non-fluorescent, but addition of Zn^{2+} ions to the solution had a skewed Gaussian shape (Fig. 3d) whereas the same spectra without Fe^{2+} was more symmetric. These suggested that the combined effect of the Zn^{2+} and Sn^{2+} was to enhance the shorter wavelength emission, whereas that of Mn^{2+} and Zn^{2+} was to simultaneously enhance at the shorter as well as longer wavelengths. This could be due to an intramolecular charge transfer (ITC) effect, due to the change in torsion of carboxylate by interactions with ions affecting the orientations of the naphthalimide with respect to the carboxylate group differed. It may be noted that upon addition of water to a DMF solution of **H_2NAPHISO** had caused showed feeble emission at 380 nm and intensity was increased with ater concentration (Fig. S18†). But the change caused was very less as compared to the one caused by Zn^{2+} ions. The flexibility on the orientation of the ring was reflected in the crystal structure of the coordination polymer, where naphthalimides had crystallographic disorder.

The changes in the emission spectra of the **H_2NAPHISO** caused by Zn^{2+} or Cd^{2+} ions were plotted against concentrations (Fig. S10†). It was found that at a lower concentration, <600 μM the changes in fluorescence intensity caused by zinc or

cadmium ions were identical. But, cadmium ions did not cause changes beyond this concentration, whereas, the zinc ions continued to cause enhancement beyond this concentration (*cf.* ~1000 μM). Hence, the two ions could not be distinguished at lower concentration, yet beyond a limiting concentration their performance on the change of emission was different.

The ^{1}HNMR spectra with assignment of the hydrogens of the **H_2NAPHISO** (in DMSO-d_6) are shown in the Fig. 4a. The peaks a, c, d was shielded upon interactions with zinc(II) acetate (diamagnetic effect of zinc ions), whereas the peak b was slightly de-shielded. Significant changes in the chemical-shift of the carboxylic O–H protons was observed with changes in the concentration of Zn^{2+} ions, suggesting carboxylate complex formation with zinc ions. As the concentration of the Zn^{2+} ions were increased, the O–H peak was broadened and was also shielded. Hence, the zinc ions primarily interacted with the carboxylic acid groups of the ligand. The chemical shifts of protons on the naphthalimide ring were also affected due to the interactions of Zn^{2+} ions through the carbonyl oxygens of the ring.

Naphthalimide derivatives in general show two reversible redox couples, due to formation of anion radical and dianion.[32] The cyclic voltammogram of the **H_2NAPHISO** had revealed a reversible peak with $E_{1/2}$ −806 mV ($\Delta E_p = 128$ mV, $i_p/i_c = 1.00$) due to anion radical (Table S2†). The anodic part of this peak was decreased systematically upon incremental addition of Zn^{2+} ions (Fig. 4b). Whereas, the cathodic peak was shifted towards lower (−ve potential) potential with decrease in cathodic current (i_c). This was attributed to the zinc ions interacting with the carbonyl of the naphthalimide unit in solution, that inhibited the anion radical formation and influenced the redox potentials of the redox-couples of the **H_2NAPHISO**.

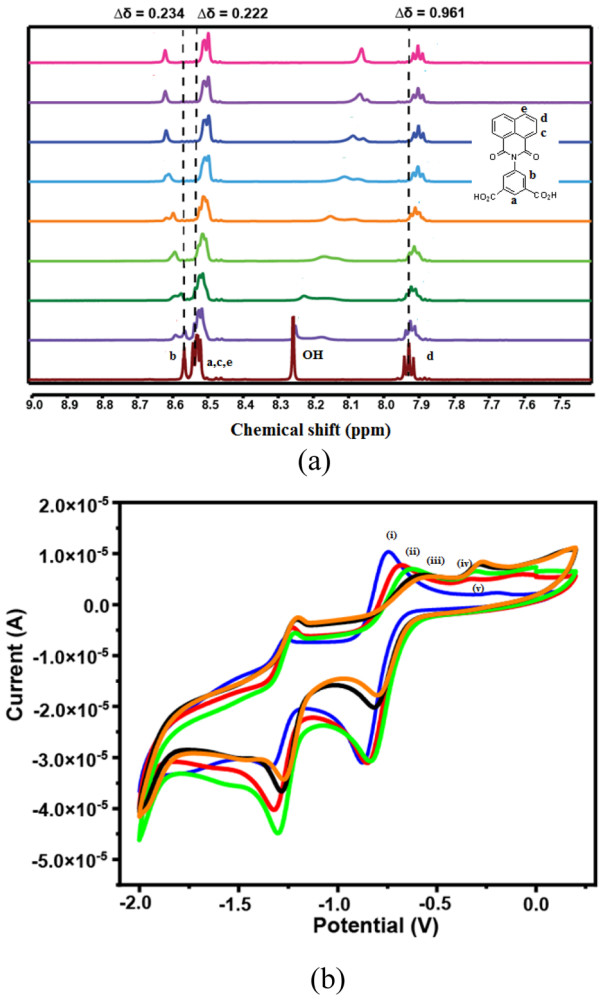

Fig. 4 (a) ^{1}H-NMR titration of the H_2NAPHISO (20 mM, in 0.5 mL DMSO-d^6) with a solution of zinc(II) acetate (50 μL in each aliquot, 20 mM in 0.5 mL DMSO). (b) Cyclic voltammogram of (i) H_2NAPHISO (1 mM, in 10 mL DMF) and, (ii)–(v) Electrochemical titration of H_2-NAPHISO by adding Zn^{2+} ions (at each time 100 μL of 1 mM in DMF), using tetrabutylammonium perchlorate as supporting electrolyte.

Interaction of the zinc-coordination polymer with Fe^{2+} ions alone or with another cation

The zinc-coordination polymer **Zn_4O-CP** was insoluble in common organic solvent, but when dispersed in DMF by sonication it showed an emission at 435 nm. As this was ON-state, fluorescence titration of the suspension prepared by dispersion of the coordination polymer with different cations were performed. The coordination polymer was stable in aqueous DMF. A control experiments of the coordination polymer in aqueous DMF after sonication with an aqueous solution of Fe^{2+} ions had showed the identical PXRD patterns with the sample of the parent compound alone (Fig. S15b†). This PXRD study also confirmed that the Fe^{2+} was not retained by the coordination polymer. The fluorescence emission spectra of fluorescent coordination polymers often get quenched by interactions with Fe^{2+} or Fe^{3+} ions.[33] In the present case, it was found that different aliquots of aqueous Fe^{2+} added to the dispersion of the **Zn_4O-CP** in DMF, there was a gradual decrease in the fluorescence emission intensity, leading to quenching of emission.

The stability of emission during the detections was confirmed by recording nine readings of emission intensities at an interval of one-minute of time and there was no change in the intensity (Fig. S9†) from the original one. This also suggested that during the detection study, there was no co- or post-precipitation of the coordination polymer from the dispersed phase. The sensing of Fe^{2+} ions in the presence of the other metal ions such as Li^+, Na^+, Hg^{2+}, Zn^{2+}, Cd^{2+}, Al^{3+} by the zinc-coordination polymers were carried out, and found that these did not quench emission. Furthermore, interference of these ions was also checked and found that they did not interfere in the quenching caused by Fe^{2+} ions. It may be noted that the influence of Li^+, Na^+, Hg^{2+}, Zn^{2+}, Cd^{2+}, Al^{3+} on the emission of the **Zn_4O-CP** were characteristic of the individual cation. Each had caused different changes as illustrated in the Fig. 5b. A set of experiments on the emission spectra of the zinc coordination polymer by adding different ions showed distinct differences in the emission change caused by effect of combinatory effect of two cations on the emission spectra of **Zn_4O-CP** and on the combinatory of the same set on the solution of **H_2NAPHISO** with externally added zinc ions. A clear distinction was seen

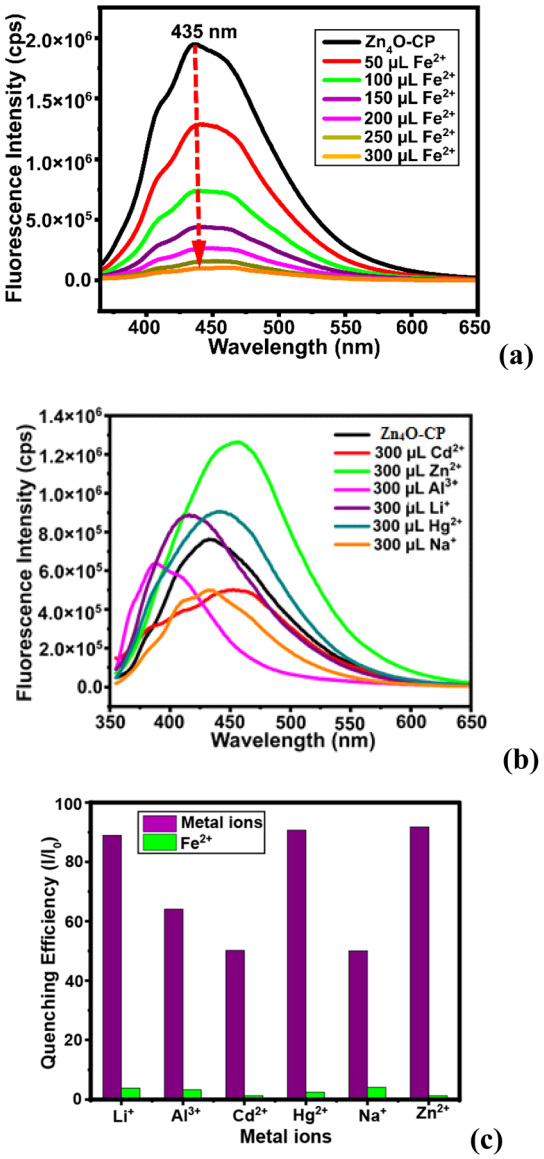

Fig. 5 (a) The fluorescence emission of a solution of the zinc-coordination polymer (3 mL suspension of 4 mg **Zn_4O-CP** in 10 mL DMF sonicated for 10 min) after each addition of Fe^{2+} ions (50 μL of 10 mM aqueous). (b) The effect of different metal ions on the emission spectra of the **Zn_4O-CP**. (c) Bar-graph of relative quenching caused by Fe^{2+} ions as compared to various other metal ions.

from the Fig. 3 and 5b of the effect. The individual ion affecting the emission spectra of the **Zn_4O-CP** are shown in the Fig. S12(a–e).† These showed that lithium ions slightly increased the intensity and changes the emission from 435 nm to 420 nm (Fig. S12a†). Whereas, sodium ion decreased the intensity without shifting the emission wavelength. The Cd^{2+}, Hg^{2+} had caused a red-shift emission wavelength (10–12 nm, Fig. S14c and d†), but Al^{3+} blue-shifted wave-length by 47 nm (Fig. S14e†). These suggest that the cations were interacting with the naphthalimide differently, which affected the intramolecular charge-transfer process by changing the orientations of the naphthalimide rings. The relative changes in intensity caused by different ions with respect to the Fe^{2+} are shown in the Fig. 5c. The value Stern–Volmer constant was calculated from the equation $I_0/I = K_{sv}[Q] + 1$; where $[Q]$ was the concentration Fe^{2+} ions, I_0 and I were the fluorescence intensity before and after the addition of Fe^{2+} ions respectively. The K_{sv} was $4.343 \times 10^6\ M^{-1}$ and the LOD for Fe^{2+} was found to be 42.57 nM. This LOD value is lower than several reported fluorescence based Fe^{2+} ion sensors (the list of substrates being too many, some selected examples are listed in the Table S3†).

The fluorescence decay profile of the **H_2NAPHISO** with Zn^{2+} ions and of **Zn_4O-CP** were triexponential, but these had large differences indicating different decay paths. The **H_2NAPHISO** with Zn^{2+} ions had a shorter decay path with life-time 0.922 ns through which only 2.06% fraction followed. Whereas, the major portion (78.54%) of the decay occurred in the case of the **H_2NAPHISO** in the presence of Zn^{2+} ions had followed a longer life-time path with a life-time 20.81 ns and also through a secondary path 6.407 ns (19.40%). On the other hand, the respective shorter life-time path of the **Zn_4O-CP** and of it with

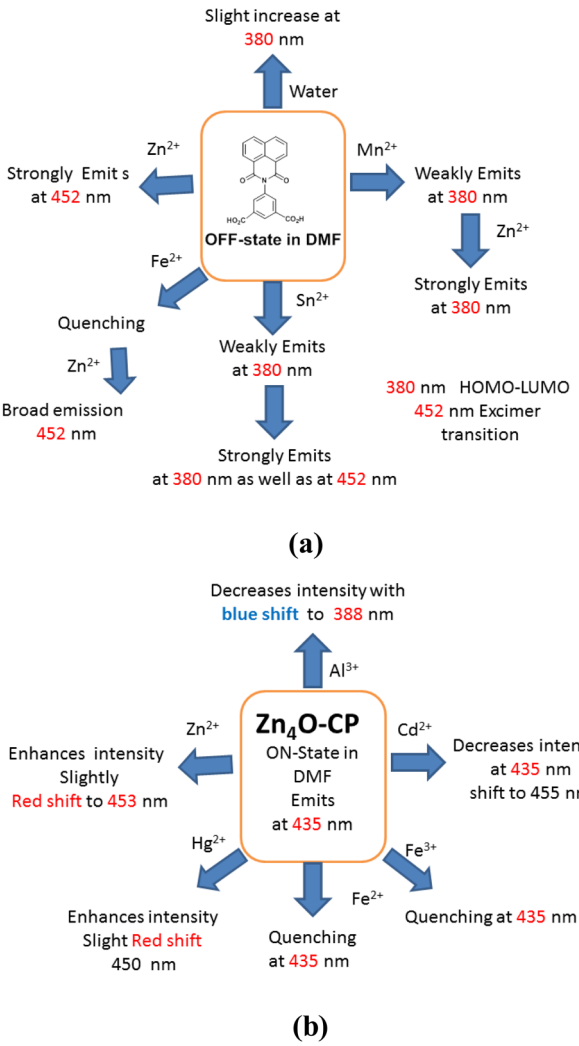

Fig. 6 (a) The combined effects of two metal ions in emission spectra of H_2NAPHISO, (b) the effects of different metal ions on the emission spectra of Zn_4O-CP.

Fe^{2+} ions were 0.896 ns (32.72%) and 0.899 ns (39.87%) respectively. These shorter life-time paths were characteristic of excimer. The **Zn_4O-CP** had two other life-times 4.226 (30.15%) and 15.22 (37.13%); whereas, the same solution with Fe^{2+} ions had 4.533 ns (29.59%) and 16.17 ns (30.54%). The amount of excimer in the two cases were similar. Two major paths in the emissions having relatively higher life-times, pointed out to TICT mechanism, occurring due to different orientations of the naphthalimide ring with the isophthalic unit.

Mechanistic aspects

The *N*-substituted naphthalimides are known to show dual emissions, the two such emissions are referred to as long-wavelength (LW) and short-wavelength (SW) emission.[34] The emission of the **H_2NAPHISO** in DMF by adding water at 380 nm (Fig. S18†) was purely singlet to singlet type transition, and it was in accordance with observation made in earlier studies on naphthalimide.[6] The divalent zinc or cadmium ion has d^{10} configuration, they interacted with the **H_2NAPHISO** in DMF to cause a chelate induced ligand to metal charge-transfer emission at 452 nm. The changes caused by different metal ions on the emission of the free ligand and the coordination polymer are shown in the Fig. 6. Solvent dependent emission peaks due to H- or J-aggregates of other zinc coordination polymers of the ligand were reported in literature.[23] In the present case, we find that **Zn_4O-CP** had a broad emission at 435 nm. The benzene dicarboxylates are known to have possibility to undergo torsional changes.[35] Upon interactions of the **Zn_4O-CP** with different metal ions stabilised different orientations of the naphthalimide rings, hence, showed distinguishable emissions upon interactions with different metals. The orientations of the naphthalimide in the polymer chain were affected by the interaction of metal ions though twisted intra-molecular charge transfer.[36] As a result red-shift or blue shift in the emission spectra of the coordination polymer by different metals was observed. Whereas, the paramagnetic effect of Fe^{2+} and Fe^{3+} contributed to the quenching of the emission spectra of the **Zn_4O-CP**.

Conclusions

A tetranuclear node of Zn_4O decorated by naphthalimide rings was accomplished and structurally characterised in a 2D-coordination polymer. The fluorescence emission of the zinc coordination polymer was selectively quenched by Fe^{2+} ions, which allowed detection Fe^{2+} ions in water with high efficiency. The emission of the coordination polymer was affected by certain cations to show partially-ON states. But, those red or blue shifts were characteristic of a cation. Whereas, the ON-state of **H_2NAPHISO** caused by Zn^{2+} ions were distinctly influenced by presence of other cations. A combined effect of two cations on the emission spectra of the free ligand was observed. The effects of those ions on the emission spectra of zinc coordination polymer were distinguishable. For example, Fe^{2+} ions did not quench emission of the ligand caused by the Zn^{2+} ions; whereas, quenching of the emission of coordination polymers was quenched by Fe^{2+} ions. A prior coordination is an important factor to control the mechanism of emission path, accordingly ligand-based emission path differed from the Zn_4O decorated based mechanistic path. These results have avenues to (a) search for new Zn_4O decorated unsymmetrical cores to have varieties in properties based on the surroundings, (b) spread emission over a wider range of wavelengths to modulate photoluminescence, and also (c) to detect specific ions in mixtures at very low concentrations.

Data availability

The data supporting this article have been included as part of the ESI.†

Author contributions

This work is carried by JS as a part of an ongoing doctoral study under the mentoring of JBB, and both have equal contributions.

Conflicts of interest

There is no conflict of interest to declare.

Acknowledgements

The authors thank the Ministry of Human Resources and Development, Govt. of India, New Delhi, for using facilities from grant no. F. No. 5-1/2014-TS.VII, and Department of Science and Technology India (Project no. SR/FST/CS-II/2017/23C and project no. SR/FST/ETII-071/2016(G)) and the central instrument facilities of IIT Guwahati for general facilities.

References

1 L. Li, J. Wang, S. Xu, C. Li and B. Dong, *Front. Chem.*, 2022, **10**, 875241.
2 (*a*) Z. Yan, Y. Cai, J. Zhang and Y. Zhao, *Measurement*, 2022, **187**, 110355; (*b*) L. Chen, L. Li, D. Wu, X. Tian, D. Xi, L. Lu, C. Yang and Y. Ni, *Sens. Actuators, B*, 2020, **303**, 127277; (*c*) H. Che, X. Tian, W. Chen, C. Dai, Y. Nie, Y. Li and L. Lu, *Microchim. Acta*, 2023, **190**, 311.
3 K. Li, Y. Chen, J. Wang and C. Yang, *Coord. Chem. Rev.*, 2021, **433**, 213755.
4 (*a*) X. Tang, Y. Wang, J. Han, L. Ni, H. Zhang, C. Li, J. Li and Y. Qiu, *Dalton Trans.*, 2018, **47**, 3378–3387; (*b*) M. Z. K. Baig, S. Pawar, R. N. P. Tulichala, A. Nag and M. Chakravarty, *Sens. Actuators, B*, 2017, **243**, 226–233; (*c*) G. U. Mahoro, J. Fernandez-Cestau, J.-L. Renaud, P. B. Coto, R. D. Costa and S. Gaillard, *Adv. Opt. Mater.*, 2020, **8**, 2000260.
5 (*a*) H. Deng, T. Wang, Y. Chen, K. Dou, X. Liu, C. Zhao, H. Zhan, C. Yang, C. Qin and Y. Cheng, *J. Phys. Chem. Lett.*, 2024, **15**, 7003–7010; (*b*) S. Shanmugaraju, C. Dabadie, K. Byrne, A. J. Savyasachi, D. Umadevi, W. Schmitt, J. A. Kitchen and T. Gunnlaugsson, *Chem. Sci.*, 2017, **8**, 1535–1546.

6 X. Wang, Z. Wang, H. Feng, C. Lin, H. Shi, Z. An, Z.-M. Su and F.-S. Liang, *Chem. Commun.*, 2022, **58**, 3641–3644.
7 (*a*) J. K. Nath, Y. lan, A. K. Powell and J. B. Baruah, *Inorg. Chem. Commun.*, 2013, **28**, 81–84; (*b*) C. Liu, W. Li, D. Du, D. Zhu and L. Xu, *J. Mol. Struct.*, 2011, **994**, 263–268.
8 (*a*) S. Banerjee, E. B. Veale, C. M. Phelan, S. A. Murphy, G. M. Tocci, L. J. Gillespie, D. O. Frimannsson, J. M. Kelly and T. Gunnlaugsson, *Chem. Soc. Rev.*, 2013, **42**, 1601–1618; (*b*) H. Yu, Y. Guo, W. Zhu, K. Havener and X. Zheng, *Coord. Chem. Rev.*, 2021, **444**, 214019; (*c*) N. Jain and N. Kaur, *Coord. Chem. Rev.*, 2022, **459**, 214454.
9 (*a*) S. Kagatikar and D. Sunil, *J. Mater. Sci.*, 2022, **57**, 105–139; (*b*) P. Gopikrishna, N. Meher and P. K. Iyer, *ACS Appl. Mater. Interfaces*, 2018, **10**, 12081–12111; (*c*) X. Wang, A. Rehman, R. M. Kong, Y. Cheng, X. Tian, M. Liang, L. Zhang, L. Xia and F. Qu, *Anal. Chem.*, 2021, **93**, 8219–8227.
10 (*a*) L. Roos, F. P. Malan and M. Landman, *Coord. Chem. Rev.*, 2021, **449**, 214201; (*b*) D. L. Reger, E. Sirianni, J. J. Horger, M. D. Smith and R. F. Semeniuc, *Cryst. Growth Des.*, 2010, **10**, 386–393; (*c*) J. Nath, A. Mondal, A. Powell and J. B. Baruah, *Cryst. Growth Des.*, 2014, **14**, 4735–4748.
11 (*a*) M. A. Kobaisi, S. V. Bhosale, K. Latham, A. M. Raynor and S. V. Bhosale, *Chem. Rev.*, 2016, **116**, 11685–11796; (*b*) Q. Li, S. Shen, L. Liang, K. Huang, D. Zheng, D. Qin and B. Zhao, *Dyes Pigments*, 2023, **219**, 111639; (*c*) Y. Zhou and L. Han, *Coord. Chem. Rev.*, 2021, **430**, 213665; (*d*) S. Shanmugaraju, C. Dabadie, K. Byrne, A. J. Savyasachi, D. Umadevi, W. Schmitt, J. A. Kitchenc and T. Gunnlaugsson, *Chem. Sci.*, 2017, **8**, 1535–1546.
12 (*a*) D. L. Reger, A. Debreczeni, J. J. Horger and M. D. Smith, *Cryst. Growth Des.*, 2011, **11**, 4068–4079; (*b*) D. L. Reger, A. P. Leitner and M. D. Smith, *Cryst. Growth Des.*, 2016, **16**, 527–536; (*c*) J. K. Nath and J. B. Baruah, *Inorg. Chem. Front.*, 2014, **1**, 342–351; (*d*) M.-H. Tremblay, A. M. Zeidell, S. Rigin, C. Tyznik, J. Bacsa, Y. Zhang, K. A. Kurdi, O. D. Jurchescu, T. V. Timofeeva, S. Barlow and S. R. Marder, *Inorg. Chem.*, 2020, **59**, 8070–8080.
13 S. Rojas-Buzo, B. Bohigues, C. W. Lopes, D. M. Meira, M. Boronat, M. Moliner and A. Corma, *Chem. Sci.*, 2021, **12**, 10106–10115.
14 C.-T. He, J.-Y. Tian, S.-Y. Liu, G. Ouyang, J.-P. Zhang and X.-M. Chen, *Chem. Sci.*, 2013, **4**, 351–356.
15 A. Morsali and J. Abedini, *Inorg. Chem. Commun.*, 2005, **8**, 460–462.
16 (*a*) H.-H. Li, Z. Niu, L. Chen, H.-B. Jiang, Y.-P. Wang and P. Cheng, *CrystEngComm*, 2015, **17**, 5101–5109; (*b*) S. Geranmayeh, A. Abbasi, A.-H. Zarnani and M. Y. Skripkin, *Polyhedron*, 2013, **61**, 6–14; (*c*) S.-J. Wang, M. A. Alavi, F. Z. Karizi, A. A. Tehrani, X.-W. Yan, A. Morsali and M.-L. Hu, *Mater. Lett.*, 2021, **287**, 129261; (*d*) S.-Q. Guo, D. Tian, X. Zheng and H. Zhang, *Inorg. Chem. Commun.*, 2011, **14**, 1876–1879.
17 (*a*) S. S. Kaye, A. Dailly, O. M. Yaghi and J. R. Long, *J. Am. Chem. Soc.*, 2007, **129**, 14176–14177; (*b*) H. Li, M. Eddaoudi, M. O'Keeffe and O. M. Yaghi, *Nature*, 1999, **402**, 276–279; (*c*) Y. Zhao, L. Wang, N.-N. Fan, M.-L. Han, G.-P. Yang and L.-F. Ma, *Cryst. Growth Des.*, 2018, **18**, 7114–7121; (*d*) M. Eddaoudi, J. Kim, N. Rosi, D. Vodak, J. Wachter, M. O'Keeffe and O. M. Yaghi, *Science*, 2002, **295**, 469–472; (*e*) I. Boldog, L. Xing, A. Schulz and C. Janiak, *Comptes Rendus Chimie*, 2012, **15**, 866–877; (*f*) A. Goswami, N. Phukan and J. B. Baruah, *Cogent Chem.*, 2015, **1**, 1060046; (*g*) S. B. Ötvös, O. Berkesi, T. Körtvélyesi and I. Palinko, *Inorg. Chem.*, 2010, **49**, 4620–4625; (*h*) R. Bertoncello, M. Bettinelli, M. Casarin, A. Gulino, E. Tondello and A. Vittadini, *Inorg. Chem.*, 1992, **31**, 1558–1565; (*i*) A. C. Tella, S. O. Owalude, S. J. Olatunji, V. O. Adimula, S. E. Elaigwu, L. O. Alimi, P. A. Ajibade and O. S. Oluwafemi, *J. Environ. Sci.*, 2018, **64**, 264–275.
18 Z. Zhang, S. Xiang, Y.-S. Chen, S. Ma, Y. Lee, T. Phely-Bobin and B. Chen, *Inorg. Chem.*, 2010, **49**, 8444–8448.
19 R. Liu, Z.-Q. Wang, Q.-Y. Liu, F. Luo and Y.-L. Wang, *Eur. J. Inorg. Chem.*, 2019, 735–739.
20 (*a*) J. Granifo, M. T. Garland and R. Baggio, *Polyhedron*, 2006, **25**, 2277–2283; (*b*) Q.-R. Fang, G.-S. Zhu, M. Xue, Q.-L. Zhang, J.-Y. Sun, X.-D. Guo, S.-L. Qiu, S.-T. Xu, P. Wang, D.-J. Wang and Y. Wei, *Chem.–Eur. J.*, 2006, **12**, 3754–3758.
21 (*a*) Y. Ma, X. Tang, M. Chen, A. Mishima, L. Li, A. Hori, X. Wu, L. Ding, S. Kusaka and R. Matsuda, *Chem. Commun.*, 2022, **58**, 1139–1142; (*b*) B. Meng, Y. Liu, Y. Xing, X. Wang and W. Li, *Inorg. Chem. Commun.*, 2016, **73**, 142–146.
22 Z. Zhou, X. Xing, C. Tian, W. Wei, D. Li, F. Hu and S. Du, *Sci. Rep.*, 2018, **8**, 3117.
23 K. Jin, N. Park, Y. Ahn, D. Seo, D. Moon, J. Sung and J. Park, *Nanoscale*, 2024, **16**, 4571–4577.
24 (*a*) K. P. Carter, A. M. Young and A. E. Palmer, *Chem. Rev.*, 2014, **114**, 4564–4601; (*b*) K. Grover, A. Koblova, A. T. Pezacki, C. J. Chang and E. J. New, *Chem. Rev.*, 2024, **124**, 5846–5929.
25 (*a*) O. M. Yaghi, M. O'Keeffe, N. W. Ockwig, H. K. Chae, M. Eddaoudi and J. Kim, *Nature*, 2003, **423**, 705–714; (*b*) J. K. Nath, Y. Lan, A. K. Powell and J. B. Baruah, *Inorg. Chem. Commun.*, 2013, **28**, 81–84.
26 D. Singh and J. B. Baruah, *Tetrahedron Lett.*, 2008, **49**, 4374–4377.
27 (*a*) Y. Li, X. Hu, X. Zhang, H. Cao and Y. Huang, *Anal. Chim. Acta*, 2018, **1024**, 145–152; (*b*) Y. Pan, J. Wang, X. Guo, X. Liu, X. Tang and H. Zhang, *J. Colloid Interface Sci.*, 2018, **513**, 418–426.
28 (*a*) C. Shu, C. Liu, M. Wu, C. Chen and M. Hong, *J. Mater. Chem. C*, 2021, **9**, 4233–4239; (*b*) R. Haldar, R. Matsuda, S. Kitagawa, S. J. George and T. K. Maji, *Angew. Chem., Int. Ed.*, 2014, **53**, 11772–11777; (*c*) Y.-F. Ma, X.-L. Liu, X.-Y. Lu, M.-L. Zhang, Y.-X. Ren and X.-G. Yang, *Spectrochim. Acta, Part A*, 2024, **309**, 123803.
29 (*a*) L. Ma, G. Liu, S. Pu, C. Zheng and C. Fan, *Tetrahedron*, 2017, **73**, 1691–1697; (*b*) N. Phukan and J. B. Baruah, *Inorg. Chem. Commun.*, 2013, **37**, 89–92.
30 (*a*) Y. Zhang, X. Chen, J. Liu, G. Gao, X. Zhang, S. Hou and H. Wang, *New J. Chem.*, 2018, **42**, 19245–19251; (*b*) K. T. Kim, S. A. Yoon, J. Ahn, Y. Choi, M. H. Lee, J. H. Jung and J. Park, *Sens. Actuators, B*, 2017, **243**, 1034–1041; (*c*) A. Bhattacharya and V. Manivannan, *J. Photochem.*

Photobiol., A, 2023, **444**, 114913; (*d*) H. Xu, Y. Xiao, Y.-G. Liu and W. Sun, *Adv. Sens. Res.*, 2024, **3**, 2300032.

31 J. Sendh and J. B. Baruah, *RSC Adv.*, 2024, **14**, 27153–27161.

32 N. Barooah, C. Tamuly and J. B. Baruah, *J. Chem. Sci.*, 2005, **117**, 117–122.

33 (*a*) Y. Cheng, M. Wu, Z. Du, Y. Chen, L. Zhao, Z. Zhu, X. Yu, Y. Yang and C. Zeng, *ACS Appl. Mater. Interfaces*, 2023, **15**, 24570–24582; (*b*) H. Nawaz, W. Tian, J. Zhang, R. Jia, Z. Chen and J. Zhang, *ACS Appl. Mater. Interfaces*, 2018, **10**, 2114–2121; (*c*) X. Zhang, Q. Ma, X. Liu, H. Niu, L. Luo, R. Li and X. Feng, *Food Chem.*, 2022, **382**, 132379; (*d*) M. Li, H. Dong, Y. Chen, W. Hao, Y. Wang, Y. Zhang, Z. Zhang, Y. Hao, Y. Zhou, F. Li and L. Liu, *Anal. Methods*, 2024, **16**, 899–906; (*e*) E. P. Asiwal, D. S. Shelar, C. S. Gujja, S. T. Manjare and S. D. Pawar, *New J. Chem.*, 2022, **46**, 12679–12685; (*f*) W. Liu, H.-L. Cui, J. Zhou, Z.-T. Su, Y.-Z. Zhang, X.-L. Chen and E.-L. Yue, *ACS Omega*, 2023, **8**, 24635–24643; (*g*) S. C. Pal, D. Mukherjee and M. C. Das, *Inorg. Chem.*, 2022, **61**, 12396–12405.

34 A. Demeter, T. Berces, L. Biczok, V. Wintgens, P. Valat and J. Kossany, *J. Phys. Chem.*, 1996, **100**, 2001–2011.

35 E. G. Meekel, T. C. Nicholas, B. Slater and A. L. Goodwin, *CrystEngComm*, 2024, **26**, 673–680.

36 C. Wang, W. Chi, Q. Qiao, D. Tan, Z. Xu and X. Liu, *Chem. Soc. Rev.*, 2021, **50**, 12656–12678.